

# Preparation and properties of Pr<sup>3+</sup>/Ce<sup>3+</sup>:YAG phosphors using triethanolamine as dispersant and pH regulator

SHIHONG TONG\*, JUNYAN ZHAO and XIU WEN

College of Sciences of Southwest Petroleum University, Chengdu, Sichuan 610500, PR China

MS received 1 September 2015; accepted 28 March 2016

**Abstract.** Pr<sup>3+</sup>/Ce<sup>3+</sup>:YAG precursors were co-precipitated using triethanolamine as dispersant and pH regulator. The different dosages of triethanolamine (*D*) vs. the properties of Pr<sup>3+</sup>/Ce<sup>3+</sup>:YAG phosphors were discussed. When *D* = 0.5 vol%, the pH of titration process was controlled in the range of ~7.94–8.16 to guarantee the uniform distribution of Al, Y, Ce and Pr in the precursors. The relatively higher pH could decrease the loss of Ce and Pr in the precursors and increase the particle size of the obtained powders, which was beneficial to the enhancement of luminescent intensity. Therefore, the precursors directly converted to pure-phase YAG at 900°C, and the phosphors calcined at 1000°C showed the best dispersity due to the dispersion effect of triethanolamine and the most excellent luminescent property. When *D* ≥ 2 vol%, although pure-phase YAG was detected, the emission intensity of the phosphors decreased due to the decrease of dispersity and purity. Moreover, the co-doped Pr<sup>3+</sup> enhanced the red emission of Pr<sup>3+</sup>/Ce<sup>3+</sup>:YAG phosphors.

**Keywords.** Co-precipitation; YAG powder; phosphor; white-light LED; ceramic.

## 1. Introduction

Yttrium aluminium garnet (YAG, Y<sub>3</sub>Al<sub>5</sub>O<sub>12</sub>) is an important host material due to its promising chemical stability, high-temperature mechanical properties and excellent optical properties [1–7]. Recently, Nd:YAG [1,2] as well as Yb:YAG [3] transparent ceramics for high power solid-state lasers and Ce:YAG phosphors for white LEDs [5–7] have attracted much attention. To synthesize YAG-based materials with better properties, it is required that YAG-based fine powders should have higher purity and higher dispersity [8–16].

Comparing with other ways for preparing YAG powders, such as solid-state reaction, sol–gel, hydrothermal treatment and so on, co-precipitation method is a relatively simpler and more cost-effective way [8–17]. The product synthesized by the co-precipitation method has shown good performance [9,10] and great potential of applications [1,7]. The choice of precipitating agent is one of the important factors affecting the properties of YAG-based powders. The common precipitating agents for preparing YAG-based powders include ammonia water [11,12], ammonium hydrogen carbonate [8–10,13–17], and urea [18]. Compared to these precipitating agents, urea solution must be heated at high temperature for release of OH<sup>−</sup> and CO<sub>3</sub><sup>2−</sup>. High temperature and slow release of OH<sup>−</sup> and CO<sub>3</sub><sup>2−</sup> were disadvantageous to prepare nanometre and good dispersible powders. Moreover, previous work showed that ammonium hydrogen carbonate exceeded ammonia water for the production of less-agglomerated and well-sinterable powders [10,19].

However, the pH of ammonium hydrogen carbonate solution was lower than ammonia water solution, the loss of cations in the precursors was more, which led to decrease in emission intensity [19]. In addition, for the same reason as ammonia water and urea, the different deposits for Y<sup>3+</sup>, Al<sup>3+</sup> and doped rare-earth ions have different solubility products, the pH of co-precipitation process using ammonium hydrogen carbonate as precipitating agent also has to be controlled to guarantee that all the metal ions are simultaneously co-precipitated and evenly distributed in the precipitated slurry according to their stoichiometric proportion in YAG-based compound [13,14]. Otherwise, there will be impurity phases appearing during the roasting process [8,15]. Also, it is completely difficult to avoid agglomeration.

To solve the above problem, Pr<sup>3+</sup>/Ce<sup>3+</sup>:YAG precursors were co-precipitated by using ammonium hydrogen carbonate (NH<sub>4</sub>HCO<sub>3</sub>) as precipitant and triethanolamine as dispersant as well as pH regulator. In this study, triethanolamine was first used as dispersant and pH regulator for the preparation of Pr<sup>3+</sup>/Ce<sup>3+</sup>:YAG phosphors. The use of triethanolamine has some advantages. First, triethanolamine could appropriately make the pH of precipitation process higher to guarantee the co-precipitation of Al, Y, Ce and Pr. Second, because of the buffer effect of the mixed solution of ammonium hydrogen carbonate and triethanolamine, the variation of the pH in the whole titration process is narrow. Thus, the pH is not necessarily to be controlled in the whole titration process. Third, suitable amount of triethanolamine played the role of dispersant, solving the problem of the serious segregation between particles. Moreover, the relatively higher pH decreased the loss of Ce and Pr in the precursors,

\*Author for correspondence (tongshihong@126.com)

which is beneficial to the enhancement of luminescent intensity. In this study, the different dosages of triethanolamine ( $D$ ) vs. the variation of pH of the solution, the phase formation, dispersity, particle size and luminescent properties of  $\text{Pr}^{3+}/\text{Ce}^{3+}:\text{YAG}$  phosphors were discussed.

## 2. Experimental

Given the chemical formula of  $(\text{Y}_{0.975}\text{Ce}_{0.02}\text{Pr}_{0.005})_3\text{Al}_5\text{O}_{12}$ ,  $\text{Pr}(\text{NO}_3)_3 \cdot 6\text{H}_2\text{O}$  (99.9%),  $\text{Ce}(\text{NO}_3)_3 \cdot 6\text{H}_2\text{O}$  (99.9%),  $\text{Y}(\text{NO}_3)_3 \cdot 6\text{H}_2\text{O}$  (99.9%) and  $\text{NH}_4\text{Al}(\text{SO}_4)_2 \cdot 12\text{H}_2\text{O}$  (99.9%) were weighted in the molar ratio of 0.015:0.06:2.925:5 and dissolved in distilled water to obtain a mixed solution, in which the concentration of  $\text{Al}^{3+}$  was 0.1 M. The precipitating agent solution, in which the concentration of ammonium hydrogen carbonate ( $\text{NH}_4\text{HCO}_3$ , A.R.) was 0.5 M, was evenly divided into four parts with 0, 0.5, 2 and 4% by volume triethanolamine added, respectively. Then the same amount of mixed solution was dropped into the four parts of precipitating agent solution at a speed of  $200 \text{ ml h}^{-1}$ , accompanied by stirring at room temperature. After titration, the suspensions were aged for 24 h, and then filtered and washed with distilled water and alcohol. After drying the precipitates at  $80^\circ\text{C}$  for 24 h in a thermostatic drier, the obtained precursors were calcined at different temperatures for 2 h.

The compositions of precipitates were investigated by the Fourier transformation infrared spectroscope (FT-IR, Perkin-Elmer Company, Spectrum one). The pH of precipitation process was monitored by a pH meter with an accuracy of 0.02. The phase formation process and microstructure of  $\text{Pr}^{3+}/\text{Ce}^{3+}:\text{YAG}$  powders were investigated by X-ray diffraction (XRD,  $D/\text{max-rA}$  model, using nickel-filtered  $\text{Cu-K}\alpha$  radiation) and the field emission scanning electron microscope (SEM, HITACHI, S-4800). Photoluminescence (PL) spectra were measured with a Hitachi Spectra-fluorimeter (F-7000).

## 3. Results and discussion

Table 1 shows the variation of the pH of ammonium hydrogen carbonate solution with different dosages of triethanolamine ( $D$ ). The initial pH is the pH of precipitating agent solution and the final pH is the pH of the solution after titration. The pH of the solution was increased with increase in  $D$ . Because of the buffer effect of the mixed solution of ammonium hydrogen carbonate and triethanolamine, the

**Table 1.** Variation of the pH of ammonium hydrogen carbonate solution with different dosages of triethanolamine ( $D$ ).

Dosages of triethanolamine ( $D$ )	0 vol%	0.5 vol%	2 vol%	4 vol%
Initial pH	7.78	8.16	8.44	8.52
Final pH	7.46	7.94	8.14	8.20

variation of the pH in the titration process was narrow, and when  $D \geq 2 \text{ vol}\%$ , the pH was increased very slowly.

Figure 1 shows the XRD patterns of  $\text{Pr}^{3+}/\text{Ce}^{3+}:\text{YAG}$  powders prepared under different experimental conditions, where the series of samples prepared under  $D = 0, 0.5, 2$  and  $4 \text{ vol}\%$  and calcined at  $1000^\circ\text{C}$  for 2 h are labelled by Y1, Y2, Y3 and Y4. It can be seen that the sample prepared under  $D = 0.5 \text{ vol}\%$  and calcined at  $900^\circ\text{C}$  for 2 h was completely transformed into pure YAG phase, which indicates that  $\text{Pr}^{3+}$  and  $\text{Ce}^{3+}$  successfully replaced  $\text{Y}^{3+}$  into the YAG lattice. As the temperature reached  $1000^\circ\text{C}$ , only the crystallinity was improved. Moreover, for those samples calcined at  $1000^\circ\text{C}$  for 2 h, except Y1 in which a few impure phases were detected, all the other samples were pure YAG phase. It seems that triethanolamine is beneficial to the preparation of pure-phase  $\text{Pr}^{3+}/\text{Ce}^{3+}:\text{YAG}$ . The reason should be that the pH of the titration process was increased by triethanolamine to guarantee the co-precipitation of  $\text{Al}^{3+}$ ,  $\text{Y}^{3+}$ ,  $\text{Ce}^{3+}$  and  $\text{Pr}^{3+}$  and the uniform distribution of  $\text{Al}^{3+}$ ,  $\text{Y}^{3+}$ ,  $\text{Ce}^{3+}$  and  $\text{Pr}^{3+}$  in the precursors.

Figure 2 shows SEM images of Y1, Y2, Y3 and Y4. Compared with Y1 prepared under  $D = 0 \text{ vol}\%$ , Y2 prepared under  $D = 0.5 \text{ vol}\%$  shows much better dispersity, which should be attributed to the dispersion effect of triethanolamine. When  $D \geq 2 \text{ vol}\%$ , the dispersity of these samples became worse, which should be attributed to that an excess of triethanolamine lost the role of dispersant and simultaneously led to the relatively higher pH resulting in the enhancement of agglomeration between particles [11]. The change of the dispersity is also proved by the particle size distribution of Y1, Y2, Y3 and Y4, as shown in figure 3. Figure 3 shows that the particle size distribution of Y2 is the narrowest. By comparing the average particle size of Y1, Y2, Y3 and Y4, as shown in table 2, it can be seen that the average particle size of Y2 obtained by the particle size distribution is closest to the result observed by SEM. The average particle sizes of Y1 and Y4 obtained by the particle size distribution are much different from the result observed by SEM, because

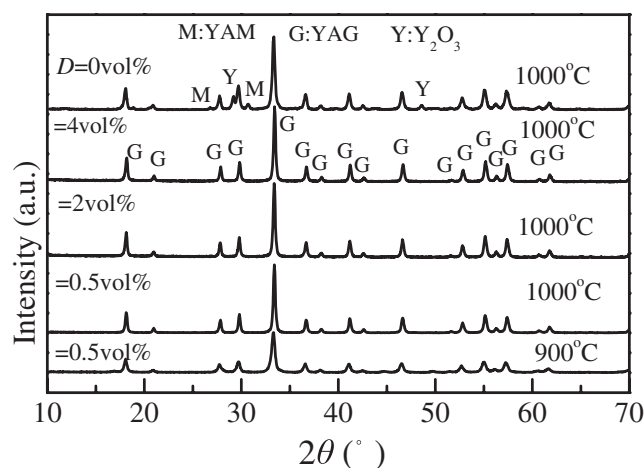


**Figure 1.** XRD patterns of YAG powders prepared under different experimental conditions.

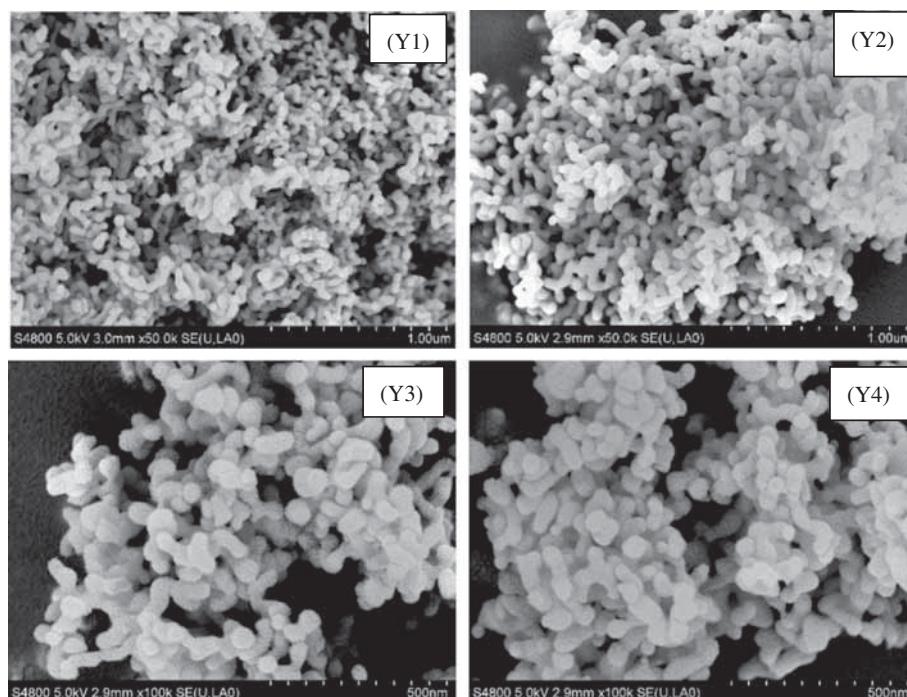


Figure 2. SEM images of Y1, Y2, Y3 and Y4.

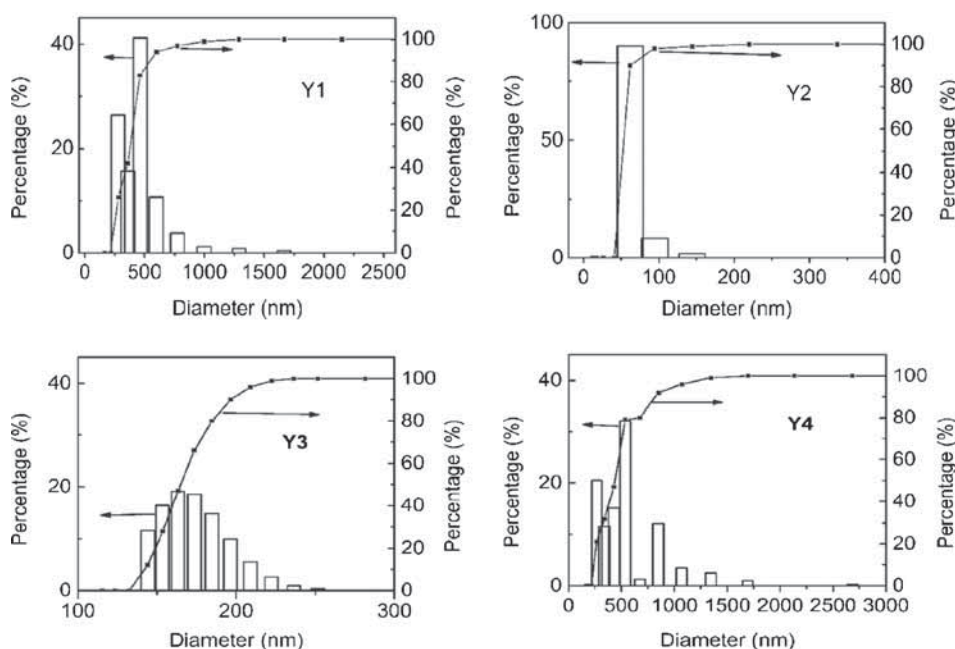


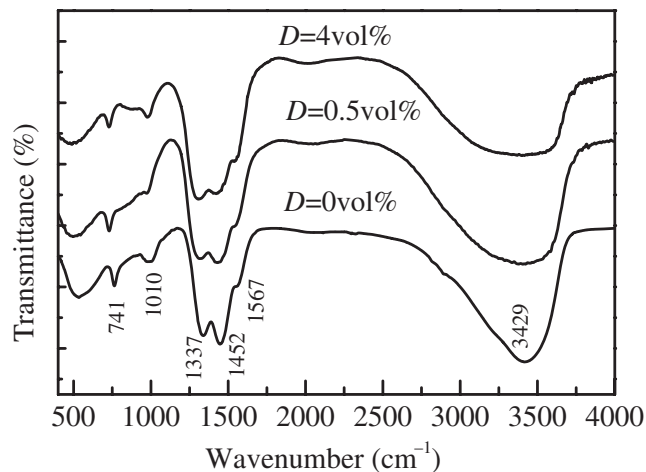
Figure 3. The particle size distribution of Y1, Y2, Y3 and Y4.

of the serious agglomeration of Y1 and Y4. It is known that the average particle size obtained by the particle size distribution should be the average size of the aggregate derived from the reunion of some particles. Therefore, from figure 3 we conclude that Y2 shows the best dispersity. In addition, as shown in figure 2, although the morphologies of all the samples are approximately spherical, the average particle size of Y2 is obviously larger than that of Y1, and the particle size increases slowly when  $D$  is increased from 0.5 to 4 vol%.

Furthermore, as shown in table 2, the crystallite size of Y1, Y2, Y3 and Y4 are 28.4, 36.7, 38.5 and 39.0 nm, respectively, which was calculated by Scherrer equation from XRD data. The result also shows that the crystallite size increases gradually with increase in  $D$ . This can be explained by the fact that the change of particle size also is related to the change of the pH. Because the increase of the pH can lead to the increase of particle size [11], the particle sizes of Y2, Y3 and Y4 are obviously larger than that of Y1. However, the pH increases

**Table 2.** Average particle and crystallite sizes of Y1, Y2, Y3 and Y4 obtained by different methods.

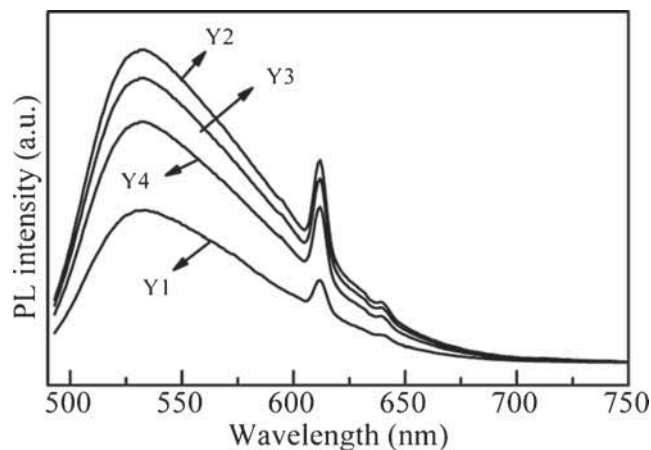
Samples	Y1 (nm)	Y2 (nm)	Y3 (nm)	Y4 (nm)
Average particle size (SEM)	~45	~53	~55	~55
Average particle size (particle size distribution)	441.5	67.5	173.0	542.2
Average crystallite size (XRD)	28.4	36.7	38.5	39.0

**Figure 4.** FT-IR spectra of the precursors synthesized by using different  $D$ .

slowly when  $D$  is above 2 vol%, in this case the increase of particle size is not obvious.

Furthermore, the change in the dispersity of these samples can also be explained by the FT-IR spectra of the precursors synthesized under  $D = 0, 0.5$  and  $4$  vol%, respectively, as shown in figure 4. It is seen that, the positions of main peaks whose vibrations are given by other literature [20] are the same in the three curves, which suggests that the triethanolamine could not change the main compositions of the precursors. However, it is found that the absorption peak at  $\sim 3429$   $\text{cm}^{-1}$  gradually becomes a wider peak in the range  $3000\text{--}3500$   $\text{cm}^{-1}$  when  $D$  is increased from 0 to 4 vol%, and the absorption intensity gradually becomes weaker, which indicates that the hydrogen bonding interaction of absorbed water is enhanced. It is supposed that the enhancement of hydrogen bonding interaction can lead to more serious agglomeration of the powders, which is consistent with the results depicted in figure 2. However, when  $D = 0.5$  vol%, the powders show the best dispersity, which indicates that the agglomeration does not increase linearly with increase in  $D$ , simply because triethanolamine is both pH regulator and dispersant.

The virtue of triethanolamine is also confirmed by the PL spectra of Y1, Y2, Y3 and Y4, as shown in figure 5. It can be seen that, the emission intensity of Y1 is the weakest, while Y2 is the strongest. When  $D = 0.5$  vol%, either increasing or reducing  $D$  will decrease the emission intensity. According to the above analysis, the use of triethanolamine increased the pH of the solution, the loss of Ce and Pr in the precursors should become less with increase in  $D$  [19]. The lower

**Figure 5.** PL spectra of Y1, Y2, Y3 and Y4 ( $\lambda_{\text{ex}} = 470$  nm).

loss of Ce and Pr led to increase in emission intensity. Also, the particle size of the samples prepared under  $D \geq 0.5$  vol% was bigger than under  $D = 0$  vol%, the small specific area brought on less surface defects, which led to decrease the possibility of nonradiative transition [19]. In addition, the purity of the samples prepared under  $D \geq 0.5$  vol% was higher than under  $D = 0$  vol%, which also led to increase in emission intensity. Therefore, the emission intensity of the samples prepared under  $D \geq 0.5$  vol% was stronger than under  $D = 0$  vol%. While  $D \geq 2$  vol%, the emission intensity was decreased, which should be attributed to the decrease of dispersity and purity of the phosphors. When  $D \geq 2$  vol%, the higher pH decreased the loss of Y, Ce and Pr, but increased the loss of Al in the precursors, which led to conclude that the molar ratio of  $(\text{Y} + \text{Ce} + \text{Pr}):\text{Al}$  was seriously over 0.6. Although the samples prepared under  $D \geq 2$  vol% were pure-phase YAG, the purity of the powders was decreased due to the amount of secondary phases ( $\text{Y}_2\text{O}_3$ , YAM and YAP), which were too few to be detected by the XRD equipment [13]. Thus,  $D = 0.5$  vol% is beneficial to the preparation of pure-phase  $\text{Pr}^{3+}/\text{Ce}^{3+}:\text{YAG}$ . Furthermore, as  $D = 0.5$  vol%, the pH of the titration process controlled in the range of  $\sim 7.94\text{--}8.16$  is beneficial to the fabrication process of  $\text{Pr}^{3+}/\text{Ce}^{3+}:\text{YAG}$  precursors, which is consistent with the conclusions of other literature [13].

It should also be remarked that, all curves exhibit a well-known yellow emission broadband peaking around 530 nm due to the transition from the lowest 5d state of  $\text{Ce}^{3+}$  to the 4f ground state of  $\text{Ce}^{3+}$ . The intense red emission line at 612 nm is due to  $^1\text{D}_2 \rightarrow ^3\text{H}_4$  of  $\text{Pr}^{3+}$ , which indicates that the co-doped  $\text{Pr}^{3+}$  has enhanced the red emission of the  $\text{Pr}^{3+}/\text{Ce}^{3+}:\text{YAG}$  phosphors. The phosphors can be used as candidate materials for the preparation of white LEDs with high colour rendering.

#### 4. Conclusion

$\text{Pr}^{3+}/\text{Ce}^{3+}:\text{YAG}$  precursors were co-precipitated by using ammonium hydrogen carbonate ( $\text{NH}_4\text{HCO}_3$ ) as precipitant

and triethanolamine as dispersant as well as pH regulator. The different dosages of triethanolamine ( $D$ ) vs. the properties of Pr<sup>3+</sup>/Ce<sup>3+</sup>:YAG phosphors were discussed. When  $D = 0.5$  vol%, the pH of the titration process was controlled in the range of  $\sim 7.94$ – $8.16$  to guarantee the uniform distribution of Al, Y, Ce and Pr in the precursors, and the precursors directly converted to pure YAG at about 900°C. The precursors synthesized under  $D = 0$  vol% transformed to YAG via a few impure phases at about 1000°C. The Pr<sup>3+</sup>/Ce<sup>3+</sup>:YAG phosphors synthesized under  $D = 0.5$  vol% showed the best dispersity due to the role of dispersant played by triethanolamine and the best luminescent property on account of the low loss of Ce and Pr, high purity, big particle size and good dispersity of the phosphors. When  $D \geq 2$  vol%, the dispersity of the powders became worse owing to the enhancement of hydrogen bonding interaction, and the emission intensity decreased due to the decrease of dispersity and purity. Moreover, the co-doped Pr<sup>3+</sup> enhanced red emission of the Pr<sup>3+</sup>/Ce<sup>3+</sup>:YAG phosphors, which can be used as candidate materials for the preparation of white LEDs with high colour rendering.

#### Acknowledgement

This research was supported by the Technology Fund of Southwest Petroleum University, under Grant 2013XJZ026.

#### References

- [1] Lu J R, Song J, Prabhu M *et al* 2000 *Japanese J. Appl. Phys.* **39** L1048
- [2] Yang H, Qin X P, Zhang J, Ma J, Tang D Y, Wang S W and Zhang Q T 2012 *Opt. Mater.* **34** 940
- [3] Tang F, Cao Y G, Huang J Q, Liu H G, Guo W and Wang W C 2012 *J. Am. Ceram. Soc.* **95** 56
- [4] Cavalli E, Esposito L, Hostasa J and Pedroni M 2013 *J. Eur. Ceram. Soc.* **33** 1425
- [5] Potdevin A, Chadeyron G, Boyer D and Mahiou R 2007 *Physica Status Solidi C* **4** 65
- [6] Nishiura S, Tanabe S, Fujioka K and Fujimoto Y 2011 *Opt. Mater.* **33** 688
- [7] Wei N, Lu T C, Li F *et al* 2012 *Appl. Phys. Lett.* **101** 061902-061902-4
- [8] Zeng M, Ma Y J, Wang Y H and Pei C H 2012 *Ceram. Int.* **38** 6951
- [9] Tong S H, Lu T C and Guo W 2007 *Mater. Lett.* **61** 4287
- [10] Li J G, Ikegami T, Lee J H, Mori T and Yajima Y 2000 *J. Eur. Ceram. Soc.* **20** 2395
- [11] Wang H Z, Gao L and Niihara K 2000 *Mater. Sci. Eng. A* **288** 1
- [12] Palmero P, Esnouf C, Montanaro L and Fantozzi G 2005 *J. Eur. Ceram. Soc.* **25** 1565
- [13] Liu W B, Zhang W X, Li J *et al* 2010 *J. Alloy Compd.* **503** 525
- [14] Sang Y H, Lv Y, Qin H, Zhang X, Liu H and Boughton R I 2012 *Ceram. Int.* **38** 1635
- [15] Li J G, Ikegami T, Lee J H and Mori T 2000 *J. Am. Ceram. Soc.* **83** 961
- [16] Xu G, Zhang X D, He W *et al* 2006 *Mater. Lett.* **60** 962
- [17] Li X, Liu H, Wang J Y, Cui H M, Zhang X D and Han F 2004 *Mater. Sci. Eng. A* **379** 347
- [18] Li J S, Sun X D, Liu S H, Li X D, Li J G and Huo D 2015 *Ceram. Int.* **41** 3283
- [19] Zhang K, Liu H Z, Wu Y T and Hu W B 2008 *J. Alloys Comp.* **453** 265
- [20] Zhao D L, Yang Q, Han Z H, Sun F Y, Tang K B and Yu F 2008 *Solid State Sci.* **10** 1028